Stabilization of a Quadrotor in Wind with Flow Sensing: Linear Modeling and Control for Attitude and Position Hold

William Craig
Graduate Research Assistant
University of Maryland
College Park, MD, USA

J.T. Lewis
Undergraduate Research Assistant
University of Maryland
College Park, MD, USA

Derek A. Paley
Willis H. Young Jr. Professor of Aerospace Engineering Education
University of Maryland
College Park, MD, USA

ABSTRACT

As quadrotor missions increase in complexity, we must also seek to increase their capability. This work addresses the ongoing challenge of flight in windy conditions through the use of a custom flow-sensing and feedback-control architecture utilizing two separate probes to measure lateral and longitudinal flow. A linear model is developed by performing system identification using CIFER® software on a 210mm quadrotor that runs customized Cleanflight firmware. A linear controller is then optimized for disturbance rejection using CONDUIT® software to meet desired handling qualities specifications. Experiments performed in an indoor gust-generation facility show improvement in both short and long time-scale gusts through the use of flow feedback.

NOTATION

e_θ	Pitch error, rad
e_q	Pitch rate error, rad/s
e_u	Longitudinal velocity error, m/s
e_x	Longitudinal position error, m
K_θ	Pitch attitude gain
K_q	Pitch rate gain
K_u	Longitudinal velocity gain
K_x	Longitudinal position gain
K_{sat}	Saturation function slope gain
M_{Δ_u}	Angular-acceleration response to wind
q	Pitch rate, rad/s
u	Longitudinal speed, m/s
$\mathbf{V}_\infty$	Wind velocity, m/s
X_{Δ_u}	Linear-acceleration response to wind
Δ_u	Longitudinal wind speed, m/s
Δ'_u	Measured longitudinal wind speed, m/s
θ	Pitch angle, rad
θ_{1s}	Longitudinal control input, %
θ_{d_1}	Outer-loop contribution to desired pitch angle, rad
θ_{d_2}	Inner-loop contribution to desired pitch angle, rad
τ_{1s}	Longitudinal time delay, s
ω_i	Angular velocity of propeller i, rad/s

Presented at the Vertical Flight Society Autonomous VTOL Technical Meeting and eVTOL Symposium 2019, Mesa, Arizona, Jan. 28–Feb. 1, 2019.

INTRODUCTION

In recent years, quadrotors have become highly capable tools with both commercial and military viability. The ability to take off and land vertically makes them attractive compared to fixed-wing Unmanned Aerial Systems (UAS) and their mechanical simplicity is an advantage compared to single-main-rotor helicopters. Current and foreseen missions, including agricultural monitoring, package delivery, and aiding in natural disasters, require stable and reliable flight in a variety of conditions.

Traditionally, stable and reliable flight for quadrotors is achieved with a trial-and-error methodology, where nominal gains are chosen based on experience, then tested in flight and adjusted as necessary. Trial and error may yield an initially unstable platform, but is often successful due to the mechanical simplicity, structural integrity, and low cost of replacement parts for quadrotors. A more rigorous approach may also be taken, using, for example, eigenvalue analysis (Ref. 1), robust control techniques (Ref. 2), or Lyapunov stability criteria (Refs. 3, 4) to provide flight stability based on system dynamics.

More recently, an approach typically used to evaluate full-scale helicopter stability and performance based on handling qualities metrics has also been pursued (Ref. 5), which involves first identifying a linear model of the vehicle, then designing a controller such that the vehicle meets the desired handling qualities specifications. A systematic approach that uses CIFER® software (Ref. 6) for frequency-domain system identification and CONDUIT® software (Ref. 7) for controller gain optimization has been used in Refs. 8, 9. We also rely on CIFER® and CONDUIT® software for model identification and controller optimization, using handling quality specifications informed by Refs. 5, 8, 9.

As quadrotors become increasingly reliable, a variety of work is being performed to extend their mission capability, including aerobatic flight (Ref. 10), sensing and perception of unknown environments (Refs. 2, 11, 12), flying with suspended loads (Refs. 13, 14), and in-flight hardware failures (Ref. 15). This work addresses flight stability of quadrotors in windy conditions, which has also been investigated by Refs. 2, 9, 11, 16–18. Gremillion *et al.* use distributed accelerometers to directly estimate the forces and moments acting on the vehicle (Ref. 2), which are then directly cancelled in control feedback. Berrios *et al.* use the Control-Equivalent-Turbulence-Input (CETI) model from Ref. 19 to design a controller that is inherently robust to disturbances with frequency content typical of turbulent wind by optimizing gains in CONDUIT® using handling qualities criteria (Ref. 9). Yeo *et al.* use flow probes to measure downwash from another quadrotor to estimate its position and avoid the resulting disturbance (Ref. 11).

The feedback control approach described here relies on onboard flow measurements in the lateral and longitudinal directions from multi-hole probes to estimate the aerodynamic forces and moments acting on the quadrotor. By combining flow measurements with inertial sensing, the controller is able to react to wind before the aerodynamic forces and moments have propagated to the rigid-body dynamics, yielding improved performance compared to using inertial sensing alone. Work validating the application of flow feedback for gust rejection using nonlinear feedback-linearization controllers was performed for a one degree-of-freedom (DOF) pitch stand in Yeo *et al.* (Ref. 16), a three DOF attitude stand in Craig *et al.* (Ref. 17), and for a six DOF free flight quadrotor in Craig *et al.* (Ref. 18). Here we use a linear control framework optimized for gust disturbance rejection with CONDUIT® software. The linear control uses flow feedback to cancel the effect of wind on the quadrotor dynamics. The flow sensor package consists of lateral and longitudinal facing probe pairs connected to a microcontroller with flexible tubing (Ref. 11), which measures differential pressure and transmits a digital signal to the onboard flight controller.

The contributions of this paper are (1) the addition of flow feedback to a linear controller optimized for gust rejection using handling qualities criteria and (2) the experimental demonstration of the benefit of adding flow feedback to a linear controller that has been designed for gust rejection. This work parallels the work in Craig *et al.*, in which a nonlinear controller was designed with flow feedback for gust disturbance rejection, but the use of an optimized linear framework is beneficial because it highlights the effect of flow feedback in an optimized, linear controller specifically designed for gust disturbance rejection.

The outline of the paper is as follows. The first section describes the software and hardware used for system identification and experimental testing. The second section describes the system identification process using CIFER® software. The third section uses the identified model to design an optimal controller based on handling qualities criterion in CONDUIT®. The fourth section shows experimental results of the six DOF quadrotor subjected to a series of gusts, and the final section summarizes the paper and discusses ongoing work.

SYSTEM DESCRIPTION

Figure 1 shows the 540g custom-built quadrotor used in this work. The vehicle has a 210mm carbon fiber Shendrones Krieger frame and a Matek F405-STD flight controller paired with a Matek FCHUB-6S power distribution board. The flight controller includes a three-axis accelerometer and three-axis gyroscope for inertial sensing. EMAX Lightning 20A ESCs control EMAX RS-2205 motors, which are paired with Gemfan 5030 five inch diameter propellers. Figure 1 also shows the differential-pressure lateral and longitudinal flow probes highlighted in red.

Fig. 1. Quadrotor used for experimental testing with flow probes highlighted in red

The overall experimental testbed is shown in Figure 2. Outer-loop sensing is performed using an 18 camera, 15' x 10' x 12' motion capture facility that records position and attitude data at 100Hz. The data recorded in motion capture is streamed locally to Matlab, which runs the outer loop position and heading controller. Desired attitude is transmitted using a 2.4

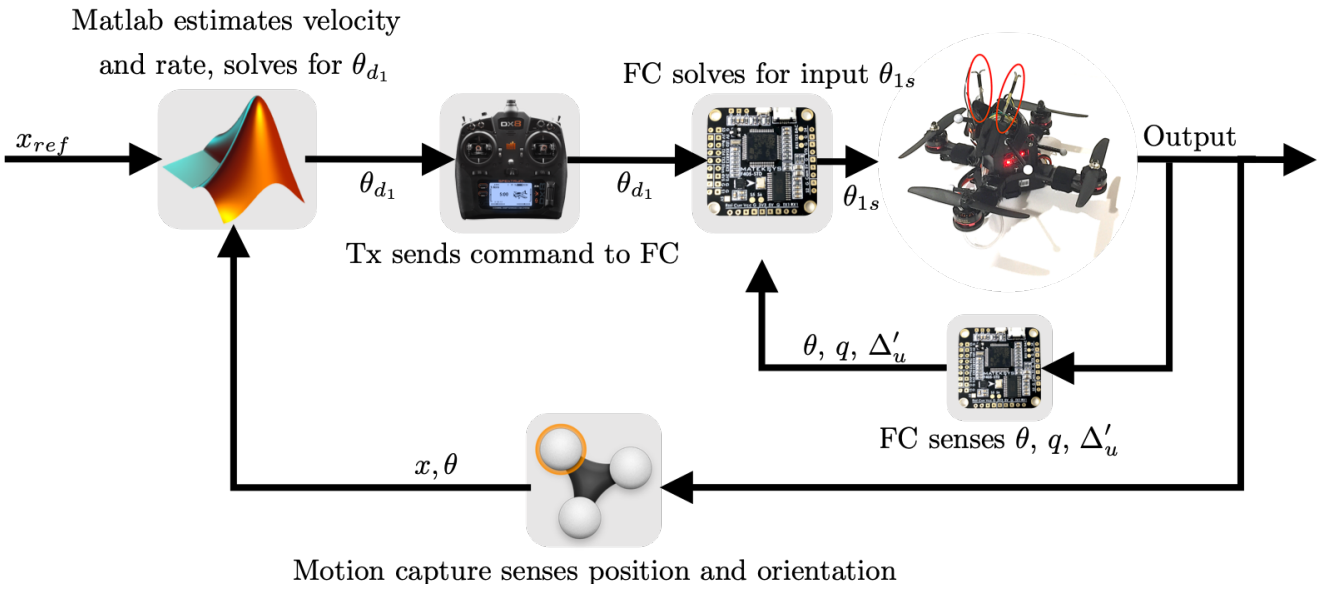

Fig. 2. Inner- and outer-loop experimental control structure for longitudinal direction

GHz Spektrum DX8 radio transmitter to the quadrotor's onboard flight controller, which solves for desired inputs. The onboard flight controller runs open-source Cleanflight software for inner-loop attitude stabilization, which has been customized to run the optimized linear controller and incorporate serial flow-sensor data. Onboard data collection is completed using the built in Blackbox feature that records states and flow data at 250Hz.

Fig. 3. Gust generation system consists of a set of eight Dyson fans behind remotely operated blinds

Gust rejection testing was completed in an indoor gust facility, shown in Figure 3, which consists of eight Dyson fans behind a set of remotely operated blinds, controlled by an Arduino through LabVIEW, that open and close to produce gusts. Two square-wave pattern gusts of different periods were tested to investigate the effects of longer and shorter frequency scales. First, the blinds were opened for five seconds at a time, giving the vehicle a chance to reach steady-state type behavior. Second, the blinds were opened for two seconds at a time, thereby not allowing the quadrotor to to reach steady state during the gust or recover fully after a gust. The quadrotor experienced a wind speed of ten knots in the five-second gust testing, and eight knots in the two-second gust testing.

MODEL IDENTIFICATION

Modeling results are presented for the longitudinal degree of freedom (the process is the same for each of the other degrees of freedom). Define inertial frame $\mathscr{I} \triangleq (O, \mathbf{e}_1, \mathbf{e}_2, \mathbf{e}_3)$ in a north, west, up orientation with O at a known point on the ground, and body frame $\mathscr{B} \triangleq (O', \mathbf{b}_1, \mathbf{b}_2, \mathbf{b}_3)$ in a forward, left, up orientation with O' at the center of mass of the quadrotor, as shown in Figure 4. In the longitudinal degree-of-freedom, u is the velocity along $\mathbf{b}_1$, q is the pitch rate along $\mathbf{b}_2$, θ is the pitch angle along $\mathbf{b}_2$, and Δ_u is the wind velocity in the $\mathbf{b}_1$ direction. Let X_u and M_u be the linear acceleration and angular acceleration response to velocity u, respectively. We also define X_{Δ_u} and M_{Δ_u} as the linear and angular acceleration response to wind Δ_u, respectively. The state-space description of the system is

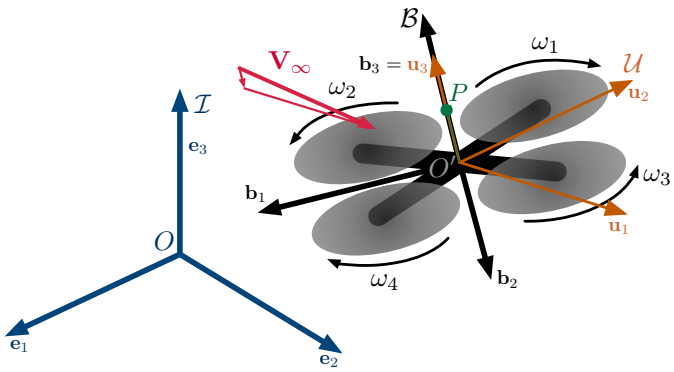

Fig. 4. Quadrotor reference frames and wind velocity

$$\begin{bmatrix} \dot{u} \\ \dot{q} \\ \dot{\theta} \end{bmatrix} = \begin{bmatrix} X_u & 0 & g \\ M_u & 0 & 0 \\ 0 & 1 & 0 \end{bmatrix} \begin{bmatrix} u \\ q \\ \theta \end{bmatrix} + \begin{bmatrix} 0 \\ M_{\theta_{1s}} \\ 0 \end{bmatrix} \theta_{1s}(t-\tau_{1s}) + \begin{bmatrix} X_{\Delta_u} \\ M_{\Delta_u} \\ 0 \end{bmatrix} \Delta_u, \tag{1}$$

$$y = \begin{bmatrix} 1 & 0 & 0 \\ 0 & 1 & 0 \\ 0 & 0 & 1 \\ 0 & 0 & 0 \end{bmatrix} \begin{bmatrix} u \\ q \\ \theta \end{bmatrix} + \begin{bmatrix} 0 \\ 0 \\ 0 \\ 1 \end{bmatrix} \Delta_u. \tag{2}$$

System identification is performed with CIFER®, which uses frequency sweeps over each channel to develop a linear model fit. Sweep profiles are performed automatically by inserting a frequency chirp into the flight-controller software. Chirps sweep from 0.62 rad/s to over 100 rad/s; an example is shown in Figure 5. Large spikes in the data are user inputs to limit translational drift.

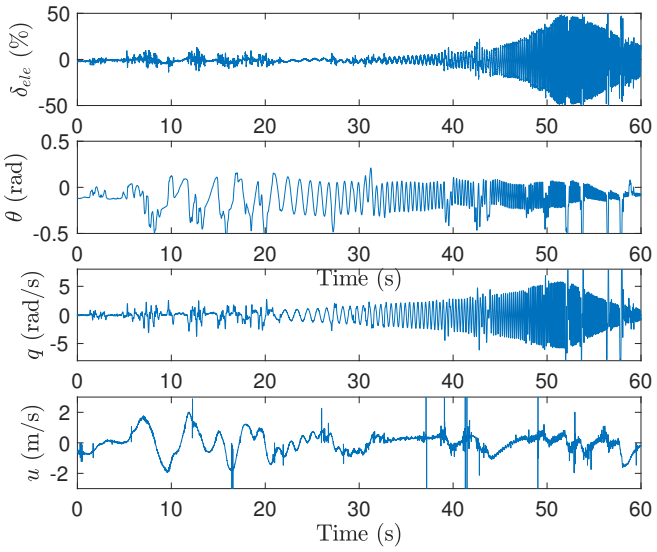

Fig. 5. Chirp data for longitudinal degree of freedom used as input to CIFER®

The resulting model fit to the flight data is shown in Figure 6. Stability derivatives are presented in Table 1, as well as Cramer-Rao bounds and insensitivities showing the level of confidence of the identification (Ref. 6). The value for X_u has been fixed based on insensitivity analysis. The model has also been validated in the time domain against independent data from separate flight tests, showing good agreement in Figure 7.

Table 1. Model parameters (see Eq. 1)

Parameter	Value	C-R %	Insensitivity %
X_u	-0.05	-	-
M_u	-10.26	4.54	1.59
$M_{\theta_{1s}}$	5.79	3.16	1.09
τ_{1s}	0.0196	5.49	2.74

We initially predicted that the effect of wind moving over the quadrotor is equivalent to the effect of the quadrotor moving forward in air, such that $X_{\Delta_u} = -X_u$ and $M_{\Delta_u} = -M_u$. However, after experimental results showed only a small effect of adding flow feedback, the gust stability derivative was adjusted based on prior force-torque measurement experimental results (Ref. 16) to be approximately twice the magnitude of the velocity derivatives. Work is ongoing to identify the gust stability derivative X_{Δ_u} using frequency domain system identification techniques.

CONTROLLER DEVELOPMENT

The quadrotor flight controller structure shown in Figure 8 uses a fast inner-loop running at 2kHz to control the attitude dynamics, and a slower outer-loop running at 100Hz to control the position and heading dynamics. The outer loop applies gains to velocity and position in proportional-integral (PI) control, and also uses a saturation function to limit the maximum desired velocity produced by the position error. The gain-adjusted velocity error is transmitted to the inner loop, where the onboard wind measurements are incorporated to produce the desired attitude. Gains are applied to attitude and rate in a proportional-derivative (PD) controller and combined with flow feedback to produce the final inputs to the motors.

To implement the PID controller, we feed back position and speed to the outer loop; and attitude, attitude rate, and wind speed to the inner loop. This example shows the development in the longitudinal direction (the process for each other degree of freedom is similar). To limit the maximum reference speed, we pass the desired position through a saturation function, i.e.,

$$u_d = \text{sat}(K_{sat}(x - x_d)), \tag{3}$$

where K_{sat} sets the slope of the saturation function. We then set the position and velocity errors

$$\begin{aligned} e_u &= u - u_d, \\ e_x &= x - x_d, \end{aligned} \tag{4}$$

and apply a PI controller to yield our desired dynamics, i.e.;

$$\dot{u}_d = -K_u e_u - K_x e_x. \tag{5}$$

Inserting Equation (5) into the dynamics (1) yields

$$\dot{u} = X_u u + g\theta + X_{\Delta_u}\Delta_u = -K_u e_u - K_x e_x. \tag{6}$$

Taking θ as our control input to the outer loop system and solving for the desired pitch angle we find

$$\theta_d = \frac{1}{g}(-K_u e_u - K_x e_x - X_u u - X_{\Delta_u}\Delta_u). \tag{7}$$

The nature of onboard versus offboard sensing necessitates splitting the desired pitch angle into separate outer- and inner-loop components, where the outer loop component θ_{d_1} uses the position and velocity data only available through motion

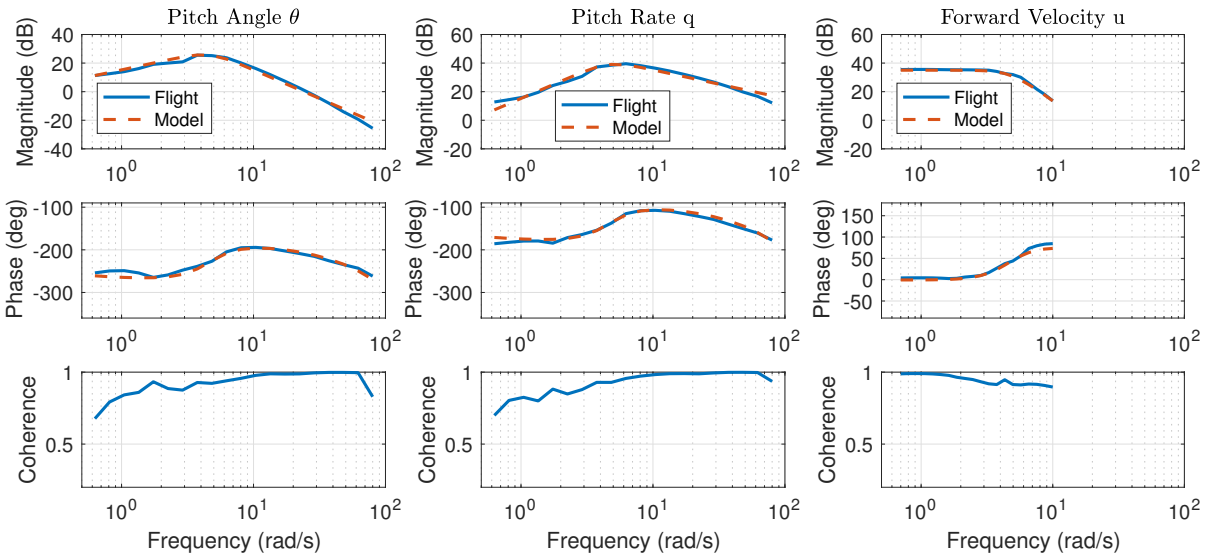

Fig. 6. Model-data agreement using stability derivatives identified in CIFER®

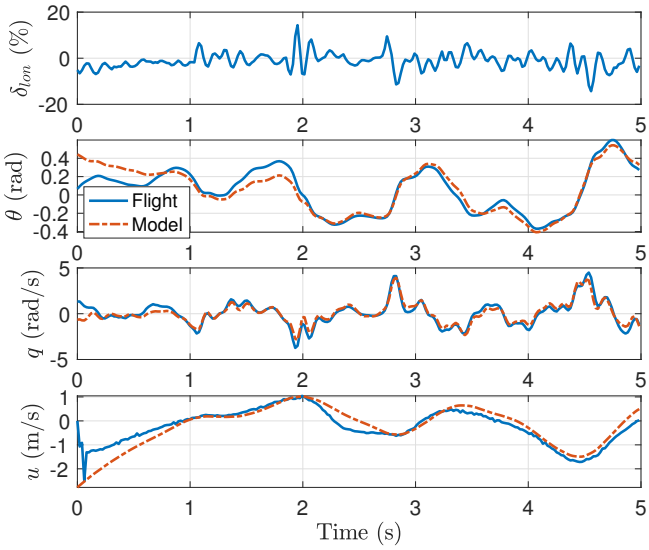

Fig. 7. Model validation against time-series data

capture, and the inner loop component θ_{d_2} uses the wind data only available from the onboard flow sensors. Note, the flow probes measure the combination of wind speed and flight speed, such that the actual measurement $\Delta'_u = \Delta_u - u$. We then calculate the stabilizing portion of the feedback, $1/g(-K_u e_u - K_x e_x)$, in the outer loop, and the dynamic cancellation portion, $1/g(-X_u u - X_{\Delta_u}\Delta_u)$, in the inner loop. Based on the initial assumption that $X_{\Delta_u} \approx -X_u$, we multiplied by the measured flow speed such that $X_{\Delta_u}\Delta'_u = X_{\Delta_u}\Delta_u - X_{\Delta_u}u \approx X_{\Delta_u}\Delta_u + X_u u$ to yield the desired value. Thus, the outer-loop component is

$$\theta_{d_1} = \frac{1}{g}(-K_u e_u - K_x e_x), \tag{8}$$

and the inner-loop component is

$$\theta_{d_2} = \frac{1}{g}(-X_{\Delta_u}\Delta'_u). \tag{9}$$

Once $\theta_d = \theta_{d_1} + \theta_{d_2}$ is identified in the inner loop, we find

$$e_\theta = \theta - \theta_d \tag{10}$$

and

$$e_q = q - \frac{d}{dt}\theta_d. \tag{11}$$

We then establish our desired dynamics:

$$\dot{q} = -K_q e_q - K_\theta e_\theta, \tag{12}$$

and substitute into the system dynamics (1),

$$\dot{q} = M_u u + M_{\theta_{1s}}\theta_{1s} + M_{\Delta_u}\Delta_u = -K_q e_q - K_\theta e_\theta. \tag{13}$$

Rearranging, with θ_{1s} as the input, the value sent to the mixer is

$$\theta_{1s} = \frac{1}{M_{\theta_{1s}}}(-K_q e_q - K_\theta e_\theta - M_u u - M_{\Delta_u}\Delta_u), \tag{14}$$

where we again account for both wind velocity and rigid body velocity using the measurement from the flow sensor to yield

$$\theta_{1s} = \frac{1}{M_{\theta_{1s}}}(-K_q e_q - K_\theta e_\theta - M_{\Delta_u}\Delta'_u). \tag{15}$$

A Simulink model of the controller in combination with the identified linear model yields optimal gains using the CONDUIT® environment. CONDUIT® requires users to choose a number of specifications relating to handling qualities stability and performance, then uses a multiobjective optimization engine to adjust gains such that each of the prescribed handling qualities specifications is achieved. More details on the CONDUIT® software are available in Ref. 7. Handling qualities are characterized as level one, two, or three, with one as the best and three as the worst. The CONDUIT® software is designed to achieve level one handling qualities for all specifications, while also minimizing

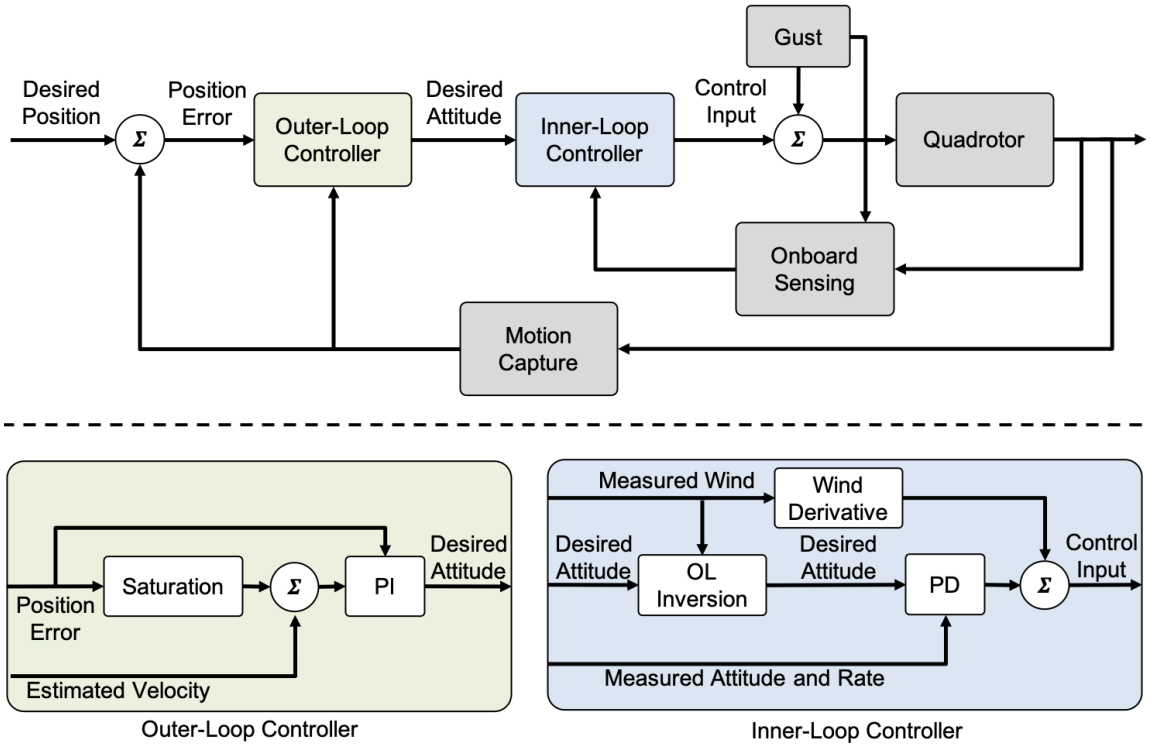

Fig. 8. Quadrotor control architecture

actuator usage. Hard specifications (H) address stability and are required to be met by the optimization, soft specifications (S) address performance based metrics and are desirable but not mandatory, and summed objective (J) specifications are designed to reduce actuator usage and are correspondingly minimized.

Nominal handling qualities specifications in CONDUIT® are designed for full-scale manned aircraft. The small size and unmanned nature of quadrotor UAS lead to different handling qualities requirements, so the CONDUIT® specifications have been adjusted based on previous work using CONDUIT® for small quadrotor UAS (Refs. 5,8). Additional adjustments were also made based on pilot feedback and flight performance. The specifications to which the gains were optimized for the longitudinal outer loop for position control are shown in Table 3, with comments addressing adjustments to handling qualities boundaries. The resulting handling qualities window is shown in Figure 9, and shows that each of the specifications meets level 1 requirements. The corresponding characteristics of the control law design are shown in Table 3.

EXPERIMENTAL RESULTS

Experimental testing was performed by subjecting the quadrotor to a series of square-wave gusts at different periods in an indoor gust generation facility. Figures 10 and 11 show displacement in the $\mathbf{e}_1$ direction as well as the flow speed experienced by the quadrotor. Figures 12 and 13 show the $\mathbf{e}_1$-$\mathbf{e}_2$ displacement on the left plot and the $\mathbf{e}_1$-$\mathbf{e}_3$ displacement on the right plot over the course of each test.

From Figures 10 and 11 we see improvement in station holding through the use of flow sensing for both tests. The longer time-scale gusts in Figure 10 show a more significant improvement, where both controllers are able to settle before and after the gusts. Without flow feedback, the quadrotor is blown back by the wind where it keeps a very consistent position until the gust ceases, and with flow feedback the quadrotor quickly compensates for the wind, and experiences only a slight movement in the direction of the wind. The shorter time scale results in Figure 11 still show an improvement through the addition of flow feedback, but highlight the benefits of designing the controller for disturbance rejection in CONDUIT® for the controller without flow feedback, and the susceptibility to noise when using flow feedback.

The linear controller produced by CONDUIT® is designed to address higher frequency turbulent wind using the disturbance rejection bandwidth specification (Ref. 20) without the use of flow sensing, and thus shows comparatively better results in the two second gusts versus testing with five second gusts. Adding flow feedback does reduce the $\mathbf{e}_1$ error in the system, however the movement appears slightly more erratic than in the longer time-scale case. The error at the beginning and end of each gust remains consistent between the longer and shorter gusts, however the shorter gusts limit the system's time to stabilize and so we see the quadrotor repeatedly overshooting the desired position as wind conditions change.

The differences in performance for the two time scales are highlighted in Figures 12 and 13, where we see that in the

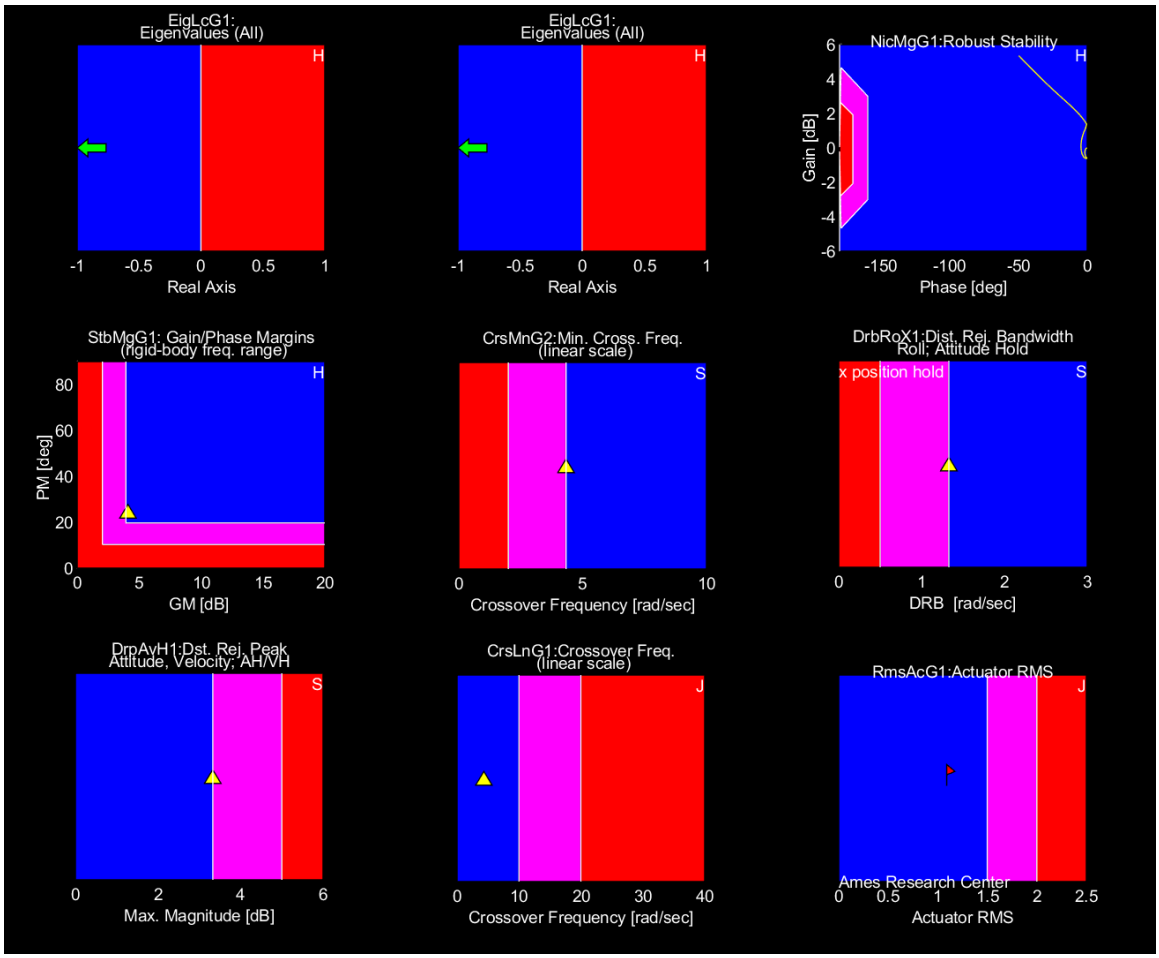

Fig. 9. CONDUIT® handling qualities window. Level one in blue, level two in pink, level three in red. Triangles and flags indicate the value of the handling quality, green arrows indicate an off-screen value, and the line in Nichols robust stability indicates the value across simultaneous changes in gain and phase.

longer time-scale gusts the systems generally maintain a tight position with or without flow sensing apart from the dynamic portion of the gust. Figure 13 shows the quadrotor unable to maintain the tight position in the presence of more rapid gusts for both cases and we also see significant motion in the $\mathbf{e}_2$ direction when flow feedback is utilized, resulting from noise and measurements in the flow signal in the lateral direction. In the longer-time-scale gusts, the $\mathbf{e}_2$ flow error reduces as the vehicle settles. However, the more dynamic wind in the shorter time-scale leads to consistent fluctuation in the $\mathbf{e}_2$ direction in addition to the response to the primary flow in the $\mathbf{e}_1$ direction. Efforts to better address noise in the flow sensors to improve performance is ongoing.

CONCLUSION

This paper describes a linear controller that has been optimized for gust rejection using CONDUIT®, based on system identification performed with CIFER®. Additionally, a custom flow probe package was used to investigate the benefits of flow feedback for gust rejection. Experiments were performed with a 210mm quadrotor system running Clean-flight software, where flow feedback yielded improvements for both short and long time-scale gusts, particularly for the longer time-scale five second gusts when the vehicle had time to settle in the wind. In ongoing work, we are investigating sensor noise to specifically reduce off-axis response and also planning outdoor flight testing.

ACKNOWLEDGMENTS

This work was supported by the University of Maryland Vertical Lift Rotorcraft Center of Excellence Army Grant No. W911W6-17-2-0004.

REFERENCES

[1]Pounds, P., Mahony, R., and Corke, P., "Modelling and control of a large quadrotor robot," *Control Engineering Practice*, Vol. 18, (7), 2010, pp. 691–699.

[2]Gremillion, G. M. and Humbert, J. S., "Disturbance rejection with distributed acceleration sensing for small unmanned aircraft systems," *AIAA Journal*, Vol. 54, (8), 2016, pp. 2233–2246.

Table 2. Design Specifications

Parameter	Description	Type	Std. Bounds?	Comments
EigLcG1	Eigenvalues	Hard	Y	
StbMgG1	Stability Margins	Hard	N	L1/L2 at 4dB, 20 deg
NicMgG1	Nichols Margins	Hard	N	L1/L2 at 160 deg
DrbRoX1	Disturbance Rejection Bandwidth	Soft	N	L1/L2 at 1.33 rad/s
DrpAvH1	Disturbance Rejection Peak	Soft	N	L1/L2 at 3.33 rad/s
CrsMnG2	Minimum Crossover Frequency	Soft	N	L1/L2 at 4.33 rad/s
CrsLnG1	Crossover Frequency	Sum. Obj.	N	L1/L2 at 10 rad/s
RmsAcG1	Actuator RMS	Sum. Obj.	Y	

Table 3. Control Law Design

Controller	Gain Margin [dB]	Phase Margin [deg]	Crossover Freq. [rad/s]	DRB [rad/s]
Pitch Attitude	9.66	21.8	25.8	11.9
Long. Position	4.10	24.8	4.33	1.33

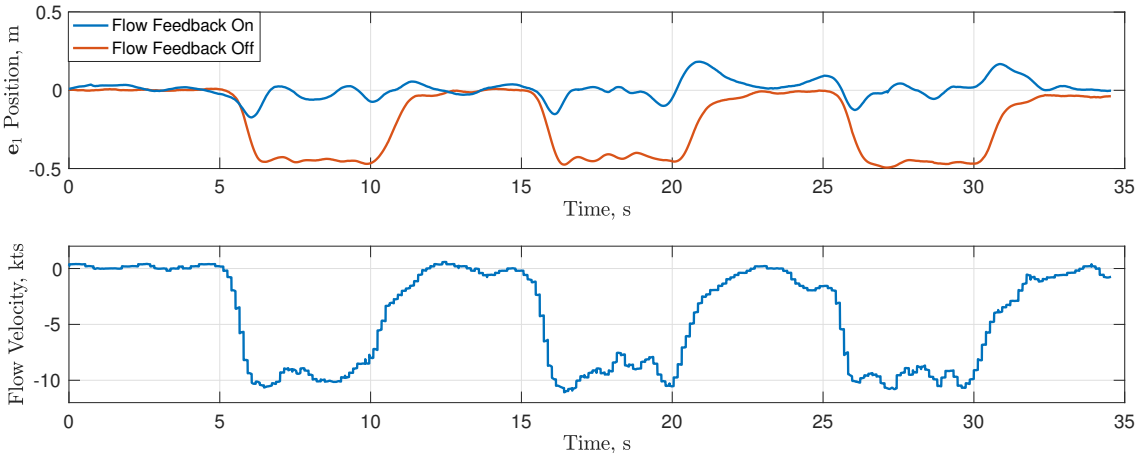

Fig. 10. Experimental quadrotor $\mathbf{e}_1$ position error in response to 5 s duration 10 kt gusts in the $-\mathbf{e}_1$ direction. Flow velocity is measured onboard using a custom flow probe.

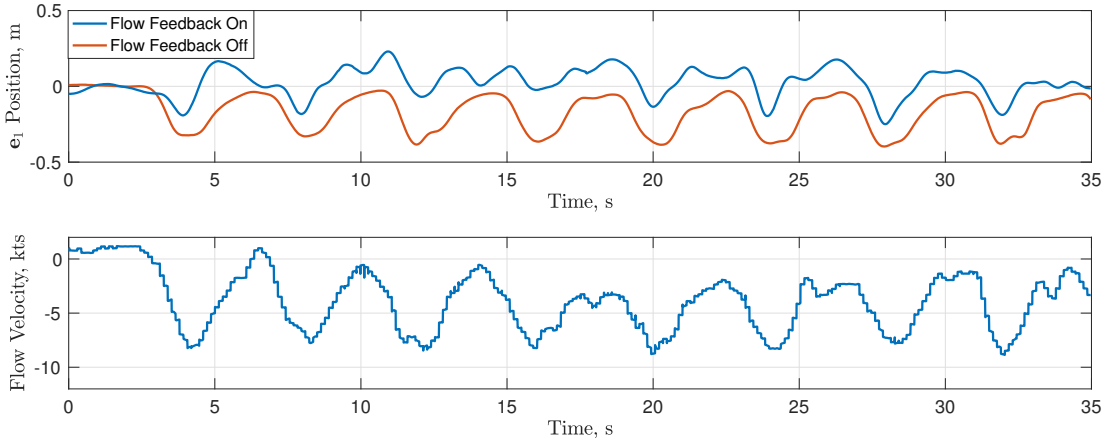

Fig. 11. Experimental quadrotor $\mathbf{e}_1$ position error in response to 2 s duration 8 kt gusts in the $-\mathbf{e}_1$ direction. Flow velocity is measured onboard using a custom flow probe.

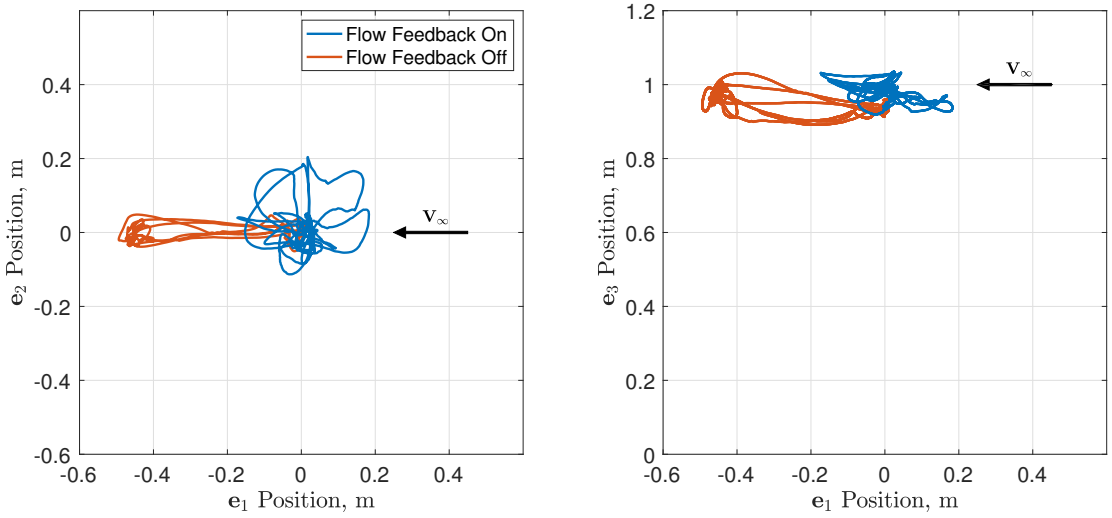

Fig. 12. Experimental quadrotor position response to 5 s duration 10 kt gusts in the $-\mathbf{e}_1$ direction.

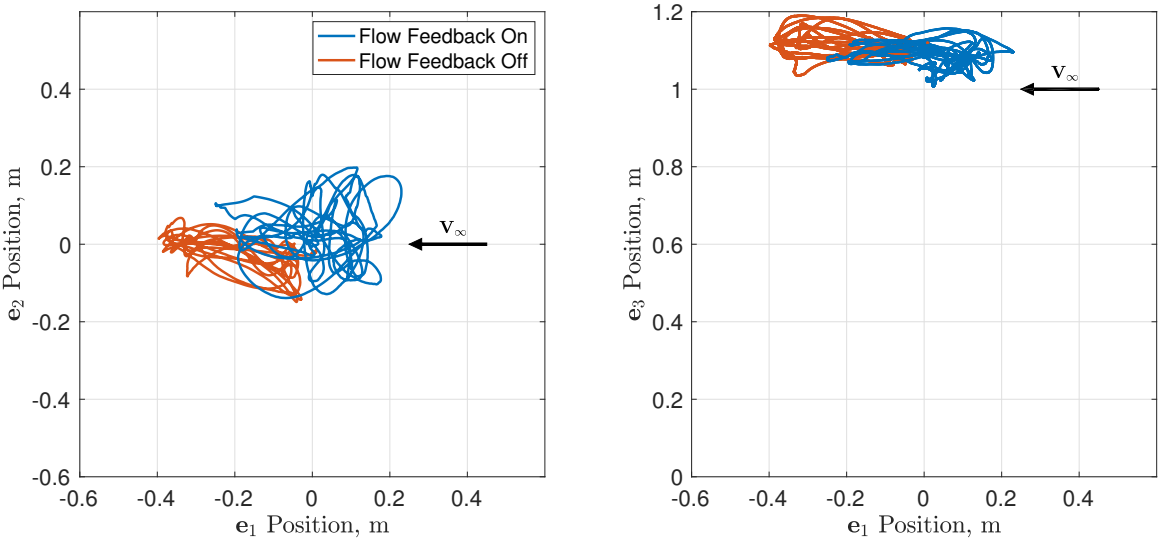

Fig. 13. Experimental quadrotor position response to 2 s duration 8 kt gusts in the $-\mathbf{e}_1$ direction.

[3]Cao, N. and Lynch, A. F., "Inner-outer loop control for quadrotor UAVs with input and state constraints," *IEEE Transactions on Control Systems Technology*, Vol. 24, (5), 2016, pp. 1797–1804.

[4]Lee, T., Leok, M., and Mcclamroch, N. H., "Geometric tracking control of a quadrotor UAV on SE(3)," IEEE Conference on Decision and Control, 2010.

[5]Cheung, K. K., Wagster IV, J. A., Tischler, M. B., Ivler, C. M., Berrios, M. G., Berger, T., Juhasz, O., Tobias, E. L., Goerzen, C. L., Barone, P. S., Sanders, F. C., Lopez, M. J. S., and Lehmann, R. M., "An overview of the U.S. Army Aviation Development Directorate quadrotor guidance, navigation, and control project," American Helicopter Society 73rd Annual Forum Proceedings, 2017.

[6]Tischler, M. B. and Remple, R. K., *Aircraft and Rotorcraft System Identification*, American Institute of Aeronautics and Astronautics, Inc., Reston, VA, second edition, 2012.

[7]Tischler, M. B., Berger, T., Ivler, C. M., Mansur, M. H., Cheung, K. K., and Soong, J. Y., *Practical Methods for Aircraft and Rotorcraft Flight Control Design*, American Institute of Aeronautics and Astronautics, Inc., Reston, VA, first edition, 2017.

[8]Wei, W., Cohen, K., and Tischler, M. B., "System identification and controller optimization of a quadrotor UAV," American Helicopter Society 71st Annual Forum Proceedings, 2015.

[9]Berrios, M. G., Berger, T., Tischler, M. B., Juhasz, O., and Sanders, F. C., "Hover flight control design for UAS using performance-based disturbance rejection requirements," AHS Int. 73nd Annual Forum, 2017.

[10]Lupashin, S., Schöllig, A., Sherback, M., and D'Andrea, R., "A simple learning strategy for high-speed quadrocopter multi-flips," IEEE International Conference Robotics and Automation, 2010.

[11]Yeo, D., Sydney, N., Paley, D., and Sofge, D., "Onboard flow sensing for downwash detection and avoidance on small quadrotor helicopters," AIAA Guidance, Navigation, and Control Conference, AIAA SciTech Forum, Paper AIAA 2015-1769, 2015.

[12]Sanket, N. J., Singh, C. D., Ganguly, K., Fermüller, C., and Aloimonos, Y., "GapFlyt: Active vision based minimalist structure-less gap detection for quadrotor flight," *IEEE Robotics and Automation Letters*, Vol. 3, (4), 2018, pp. 2799–2806.

[13]Lee, T., "Geometric control of quadrotor UAVs transporting a cable-suspended rigid body," *IEEE Transactions on Control Systems Technology*, Vol. 26, (1), 2018, pp. 255–264.

[14]Pereira, P. O. and Dimarogonas, D. V., "Control framework for slung load transportation with two aerial vehicles," IEEE Conference on Decision and Control, 2018.

[15]Lanzon, A., Freddi, A., and Longhi, S., "Flight control of a quadrotor vehicle subsequent to a rotor failure," *Journal of Guidance, Control, and Dynamics*, Vol. 37, (2), 2014, pp. 580–591.

[16]Yeo, D. W., Sydney, N., and Paley, D. A., "Onboard flow sensing for multi-rotor pitch control in wind," *Journal of Guidance, Control, and Dynamics*, Vol. 41, (5), 2018, pp. 1193–1198.

[17]Craig, W., Passe, B. E., Yeo, D., and Paley, D. A., "Geometric attitude control of a quadrotor in wind with flow sensing and thrust constraints," Submitted to *IEEE Transactions on Control Systems Technology*, 2018.

[18]Craig, W., Yeo, D., and Paley, D. A., "Geometric control of a quadrotor in wind with flow sensing and thrust constraints: Attitude and position control," AIAA SciTech Forum, Paper AIAA 2019-1192, 2019.

[19]Juhasz, O., Lopez, M. J., Berrios, M. G., Berger, T., and Tischler, M. B., "Turbulence modeling of a small quadrotor UAS using system identification from flight data," Paper January, AHS Technical Meeting on VTOL Unmanned Aircraft Systems, 2017.

[20]Berger, T., Ivler, C. M., Berrios, M. G., Tischler, M. B., and Miller, D. G., "Disturbance rejection handling qualities criteria for rotorcraft," AHS Int. 72nd Annual Forum, 2016.